BUTTERWORTH HEINEMANN

Mechanisms of heat transfer enhancement and slow decay of swirl in tubes using tangential injection

F. Chang and V. K. Dhir
Mechanical, Aerospace, and Nuclear Engineering Department, School of Engineering and Applied Science, University of California, Los Angeles, Los Angeles, CA, USA

The turbulent flowfield in a tube heated uniformly from the wall has been experimentally studied when fluid is injected tangentially. The experiments were conducted by injecting air through injectors placed on the periphery of a 88.9-mm inside diameter and 2.5-m long acrylic tube. Six injectors of 22.23-mm inside diameter were used and tangential to total momentum flux ratio of 2.67 was obtained in the experiments. Temperature profiles were measured with a resistance thermometer probe. Profiles for mean velocities in the axial and tangential directions, as well as the Reynolds stresses were obtained using a single rotated straight hot wire and a single rotated slanted hot wire anemometer. No significant difference in mean velocities and Reynolds stresses were found between the adiabatic experiments and diabatic ones. Two major mechanisms for enhancement of heat transfer are identified: (1) high maximum axial velocity near the wall produces higher heat flux from the wall; and (2) high turbulence level in the middle region of the tube improves mixing and, thus, the rate of heat transfer. Furthermore, it is observed that both the kinetic energy of the mean flow and the turbulence level decrease as swirl decays. However, during the decay process, the high turbulence-energy-production from Reynolds stresses is necessary to transfer the kinetic energy of the mean flow to the turbulence energy. This high turbulence-production, in turn, slows down the rate of decrease of the turbulence level. As a result, the swirl and the heat transfer enhancement are preserved for a long distance.

Keywords: swirl flow; heat transfer enhancement; turbulence

Introduction

The need for high-performance thermal systems stimulates interest in developing techniques for heat transfer augmentation. Improvement in heat transfer coefficients is desirable because it can reduce the size of a heat exchanger for a given thermal load or increase the capacity of a heat exchanger. In the past, many schemes for enhancing heat transfer have been studied. The use of swirl flow is among the most promising techniques for heat transfer augmentation. Swirl flow is generally referred to as a vortical flow with an axial velocity component. Three-dimensionality and streamline-curvature make the swirl flow a typical complex flow. A detailed description of confined swirl flows and their potential in heat transfer augmentation have been given by Razgaitis and Holman (1976).

A number of methods have been used to generate swirl flow in a tube, including twisted tape inserts, coiled wires, propellers, inlet guided vanes, and tangential injection of the fluid. Some of these methods generate swirl continuously along the entire length of the test section; whereas, others are placed at the inlet with the decay of swirl along the tube. Twisted-tape inserts have been used as a continuous swirl generator in many industrial applications. Twisted tapes, when inserted in tubes, tend to promote turbulence and mixing. Better mixing, coupled with the fin effect of the twisted tapes, results in improvement in heat transfer. Data by Junkhan et al. (1985) for Reynolds numbers from 5,000 to 30,000 showed heat transfer enhancement in the range of 65 to 175 percent. However, friction factor showed an increase between 160 and 1,100 percent. Thus, with continuous swirl generation, high heat transfer enhancement is generally accompanied by an even higher increase in pressure drop resulting in increased operational cost.

Instead of the continuous swirl generation, the decay of a turbulent swirl flow in a tube using a twisted tape at the inlet was investigated by Kreith and Sonju (1965). Data with water in a 1 in. pipe showed that swirl decayed to 10–20 percent of its initial intensity in a length of about 50 diameters. Blackwelder and Kreith (1970) experimentally investigated the heat transfer and pressure drop characteristics of a decaying swirl, using a twisted tape as inlet swirl generator. It was found that in the initial 20–30 diameters downstream from the end of the tape inducer, the augmentation of the heat transfer coefficient per unit pumping power exceeded considerably that possible in a continuous swirl flow. Klepper (1973) also used the combination of a twisted tape followed by a swirl decay

Address reprint requests to Dr. Dhir, School of Engineering and Applied Science, UCLA, 405 Hilgand Avenue, Los Angeles, CA 90024, USA.

Received 23 May 1994; accepted 22 November 1994

This work received support from Gas Research Institute under Contract No. 5086-260-1535.

Int. J. Heat and Fluid Flow 16: 78–87, 1995

655 Avenue of the Americas, New York, NY 10010

0142-727X/95/$10.00
SSDI 0142-727X(94)00016-6

region to improve heat transfer. It was found that a decaying swirl region downstream of a twisted tape may provide heat transfer enhancement at a relatively smaller pressure drop penalty. Thus, optimum designs of heat exchangers with tape-induced swirl must rely on combination of continuous and decaying swirl flows.

Kreith and Margolis (1959) proposed that heat transfer can be enhanced by introducing swirl flow in the heat exchanger with tangential injection of the fluid at various locations along the tube axis. However, they never tested the concept. Guo and Dhir (1987) studied the effects of injection-induced swirl on single- and two-phase heat transfer using water as the test fluid. They found as much as sixfold increase in the local single-phase heat transfer coefficient. The heat transfer coefficient was found to increase to a very large value just downstream of the injection location, then it decreased nearly exponentially with distance. On a constant pumping power basis, a net enhancement of about 20 percent could be achieved in their experiments. The ratio of the injected tangential momentum flux to the axial momentum flux rather than Reynolds number was found to be the deciding factor in heat transfer augmentation.

Dhir and Chang (1992) studied the heat transfer enhancement using tangential injection. The experiments were conducted with air as the test fluid. They showed that with tangential injection, an average enhancement of 35 to 40 percent in heat transfer was obtained on a constant pumping power basis. It was also found that the enhancement is strongly dependent on the ratio of the rate of tangential to axial momentum flux as shown in Figure 1 but is weakly dependent on Reynolds number. Tube diameter and number of injectors do not affect the heat transfer, and, as such, are not independent parameters.

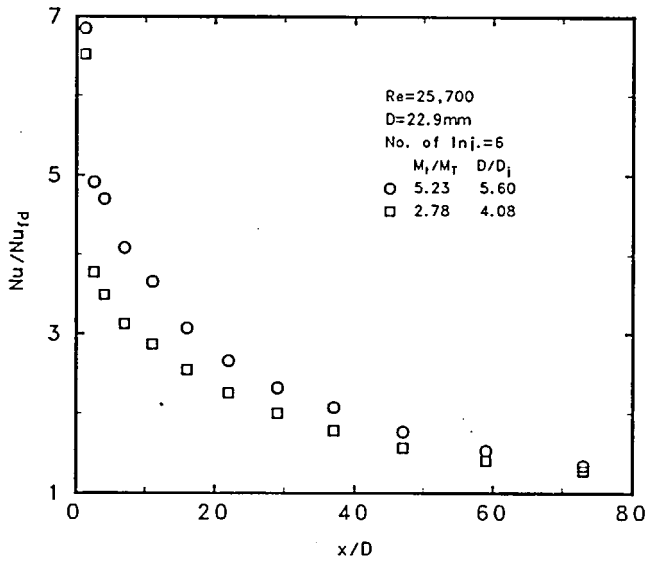

Figure 1 Heat transfer enhancement

Chang and Dhir (1994) experimentally investigated turbulent flowfield in tangentially injected swirl flow. Air was used as the

Notation

A	cross-sectional area of the test section
A_j	total cross-sectional area of all injectors
c_p	specific heat of the fluid
D	inside diameter of the test section
D_j	inside diameter of the injectors
e	dissipation rate
E_k	nondimensionalized average kinetic energy over the cross-section
k	turbulence energy
k_f	thermal conductivity of the fluid
L	total length of the test section
$\dot{m}_T$	total mass flow rate at the test section exit
$\dot{m}_t$	total mass flow rate of the injected fluid
M_T	total momentum flux rate of the axial flow
M_t	tangential momentum flux rate of the injection fluid
N	number of injectors
Nu	local Nusselt number
Nu_{fd}	fully developed Nusselt number
Nu_0	local Nusselt number in the absence of turbulence in the free stream
P	static pressure
q^2	twice energy of turbulence
$(\overline{q^2})_{av}$	cross-sectional average value of twice energy of turbulence
q_w	average wall heat flux
r	coordinate in the radial direction
R	tube radius
Re	Reynolds number
t	temperature fluctuations
$\overline{t^2}$	mean square of temperature fluctuations
T	temperature of the fluid
T_b	bulk temperature of the fluid
T_{in}	temperature of the fluid at the inlet
Tu	total turbulence intensity
T_w	wall temperature
u	velocity fluctuation in the axial direction
$\overline{u^2}$	mean square of velocity fluctuation in the axial direction
$\overline{uv}$	Reynolds stress component
$\overline{uw}$	Reynolds stress component
U	mean axial velocity
U_{av}	bulk axial velocity
U_{max}	maximum axial velocity
U_0	free-stream velocity
v	velocity fluctuation in the radial direction
$\overline{v^2}$	mean square of velocity fluctuation in the radial direction
$\overline{vw}$	Reynolds stress component
V	mean radial velocity
w	velocity fluctuation in the tangential direction
$\overline{w^2}$	mean square of velocity fluctuation in the tangential direction
W	mean tangential velocity
x	coordinate in the axial direction

Greek

θ	coordinate in the tangential direction
μ_f	viscosity of the fluid
Ω	swirl intensity

test fluid. Using a single rotated straight hot wire and a single rotated slanted hot wire anemometer, profiles for mean velocities in the axial and tangential directions, as well as the Reynolds stresses were obtained. Axial velocity profile showed existence of flow reversal region in the central portion of the tube and an increased axial velocity near the wall. Tangential velocity profiles had local maxima, the location of which moved radially inward with distance. The decay of swirl intensity was correlated with the axial distance and the initial momentum flux ratio at Reynolds number of 12,500. The dramatic increase of turbulence intensities was attributed to the destabilizing distribution of angular momentum in the free vortex zone (Bradshaw, 1973) and the large shear stress near the boundary of the reverse flow. Reynolds stress data showed an anisotropy in eddy viscosity.

Razgaitis and Holman (1976) have discussed several possible mechanisms of the heat transfer augmentation in swirl flow. One of the mechanisms discussed is the recirculation zone at the center of the tube. The recirculation zone improves the convective heat transfer because it increases the effective axial Reynolds number by reducing the cross-sectional flow area. The increased mean velocity, in turn, produces larger temperature gradients and a higher heat transfer rate. Even in the swirl flow with low swirl intensity, in which no recirculation is found, it is expected that the axial velocity near the wall is increased because of tangential injection.

Another heat transfer mechanism mentioned by Razgaitis and Holman (1976) is that the destabilizing distribution of angular momentum in the free vortex zone predicted from Rayleigh criterion improves transfer of heat and momentum. For turbulent flows, Bradshaw (1973) noted that velocity fluctuations were amplified near a concave wall and resulted in improved convection of heat and momentum at an outer tube wall in both curved and vortex swirl flows. Chang and Dhir (1994) showed that the turbulence production from the radial gradient of the tangential velocity was dramatically increased in the annular region over which the angular momentum decreased with the radius. As a result, turbulence intensities were increased significantly, which in turn lead to a better mixing.

The thermal instability was also discussed as a possible mechanism of heat transfer augmentation in swirl flow by Razgaitis and Holman (1976). A thermally stratified layer resulting from the centrifugal force promotes mixing by pushing the cold (heavy) fluid toward the wall and hot (light) fluid toward the center when the tube wall is heated.

One attractive feature of the heat transfer augmentation technique using tangentially injected swirl flow is the slow decay of the heat transfer enhancement. As shown in Figure 1, Dhir and Chang (1992) observed that even at 70 hydraulic diameters from the injection location heat transfer coefficient for an initial momentum ratio of 2.78 and a Reynolds number of 25,700 is still 25 percent higher than that for fully developed turbulent flow. In contrast, heat transfer data for hydrodynamically and thermally developing axial flow (Mills 1962) showed that the heat transfer enhancement in the entry length region died down at 10–15 hydraulic diameters. Slow decay of swirl results in high overall heat transfer enhancement.

Different behavior of the swirl flows with high swirl and low swirl were found by Weske and Sturov (1974). The required distance to reach the fully developed flow, where the flowfield variables did not change with the axial distance, was reduced by the swirl flow when the swirl intensity was small. However, for flows with high swirl intensity, the turbulence intensities increased steeply, and the distance required to reach the fully developed flow was also increased. It is apparent that different mechanisms determine the approach to fully developed flow conditions for swirl flows with high swirl intensity and low swirl intensity (or the developing axial flow). These mechanisms have yet to be investigated.

Data for temperature field and flowfield under diabatic conditions are needed to assess the combination of various mechanisms. To the authors' knowledge, no data are reported in the literature on temperature distributions, velocity distributions, and Reynolds stresses in heated decaying swirl flows. In the present work, measurements of velocity profiles and Reynolds stresses in tangentially injected swirl flow under diabatic conditions are reported. Data obtained in the present work, as well as in the earlier work (Dhir and Chang 1992; Chang and Dhir 1994) are used to investigate the mechanisms of heat transfer enhancement and slow decay of swirl.

Experimental apparatus and procedure

The experimental set-up used to study the turbulent flowfield in the tangentially injected swirl flow in a tube is shown in Figure 2. The test section consists of a clear acrylic tube of 3.5 in. (88.9 mm) inside diameter, 0.125 in. (3.2 mm) wall thickness, and 1.5-m long, which is the same as that used in the authors' earlier work (Chang and Dhir 1994). Air was injected tangentially through a set of tubular injectors made of tubing of the same material as the test section. Installation details of tubular type of injectors are shown in Figure 3. Six injectors of 0.875 in. (22.23 mm) inside diameters are used in the experiments. In the reported experiments, injectors were placed near the tube inlet. The fluid entering tangentially was evenly distributed among the injectors and was controlled with float-type flow meters. The ratio of the rate of momentum flux through the injectors to the rate of total momentum flux through the test section is defined as follows:

$$M_t/M_T = \dot{m}_t^2/\dot{m}_T^2 \; A/A_j \qquad (1)$$

where $\dot{m}_t$ and $\dot{m}_T$ are the total mass flow rates through the injectors and the test section, respectively, and A and A_j are the cross-sectional area of the test section and the total cross-sectional area of the injectors, respectively. In the present work, all the fluid was injected tangentially; hence, the ratio $\dot{m}_t/\dot{m}_T$ is equal to unity. Tangential to total momentum flux ratio of 2.67 was obtained in the experiments.

To measure the temperature and flowfield when the test section is heated, 42.4 in. (1.08 m) of the test section starting from the location near the inlet was heated with an Omega heating tape wrapped around the test section. The tape was heated with power from an AC transformer that converts the

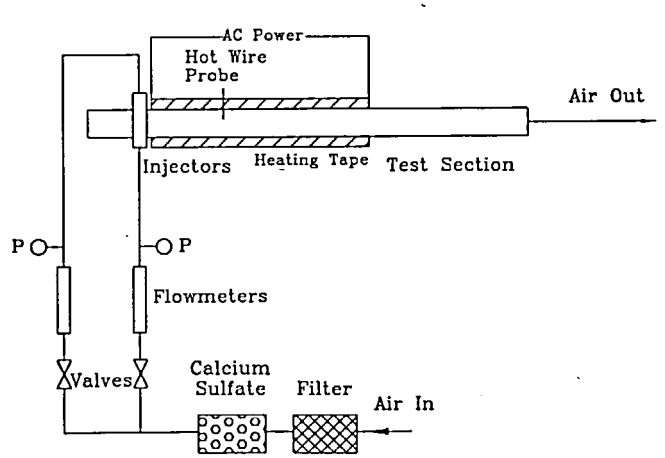

Figure 2 Schematic diagram of experimental apparatus

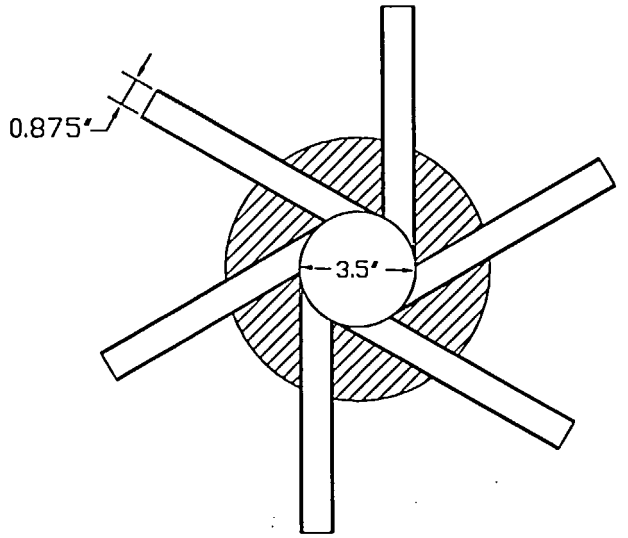

Figure 3 Details of injectors

ordinary 115 V/60 Hz line voltage into an adjustable AC source. The power was kept at about 250 W, so that the bulk temperature difference between the inlet and the exit was about 15°C and the exit temperature was well below the melting temperature of acrylic tube. To measure the temperatures of the outer wall, six K-type thermocouples were attached at the outer surface of the tube. The thermocouples were installed along the tube axis at 3, 6, 7, 8, 9, and 10 hydraulic diameters from the injection location. Six additional thermocouples were embedded in the tube wall near the tube inner surface. The temperatures at the inner wall were obtained by extrapolation of these measured temperatures.

Dantec 55P31 resistance thermometer probe was used to measure the temperature field in swirl flow. The probe has a 1-μm diameter and 0.4-mm long platinum wire and was operated with a set of Dantec 56C01 CTA and a 56C20 temperature bridge. The accuracy of 55P31 probe is ± 0.1°C. Zero point of the probe signal was checked in every set of experiments to reduce zero drift effect. The probe support was aligned in the radial direction by a traversing mechanism mounted on a slot on the tube wall. The probe could be moved radially to the position where the measurements were to be made. Dantec 55P11 straight wire and 55P12 slanted wire were used to measure mean velocities, turbulence intensities, and Reynolds stresses in the injected swirl flow. To measure the flowfield when the test section is heated, Dantec 55P11 and 55P12 probes needed to be calibrated at various temperatures. The probes were calibrated at 21.8°, 26.0°, 30.0°, 35.0°, and 39.6° in the orientation in which the velocity was perpendicular to the plane of the wire and the prongs. The flowfield was measured by following the same procedure as used in the adiabatic experiments (see Chang 1994) except that the effective cooling velocities at a specific fluid temperature were obtained from the interpolation of the calibration curves for various temperatures. The nonlinearity in temperature response is much smaller than that in velocity response, because such an error made in reducing the data by using average temperatures is considered to be small. Because the hot wire cannot sense the reverse flow, a total pressure probe was used to estimate the approximate flow angle before hot wire measurements were made.

The experiments were initiated by adjusting the flow rates to the desired values. The power of the heating tape was increased to about 250 W. This gave a heat flux of about 860 W/m^2 on the inner wall. Wall temperatures were obtained from the thermocouple readings. Data were collected at 15-min intervals until no change in measured temperatures was observed. Once the steady state was reached, wall temperature data were recorded, and the fluid temperatures were measured with Dantec 55P31 probe. This temperature field was later used to interpolate the response of Dantec 55P11 and 55P12 hot wire probes in a non- isothermal flowfield.

The experiments were restarted by adjusting the flow rate and power to the values for which the temperature field measurements were made. Dantec 55P11 and 55P12 were used separately to measure the flowfield. Interpolation of the calibration data was used to determine the hot wire response. The axial velocity obtained in this manner is estimated to be accurate to ± 7 percent of the bulk axial velocity, defined as the average axial velocity over the cross-section, while the tangential velocity is accurate to ± 13 percent of the bulk axial velocity (for details see Chang 1994). The bulk temperature can be obtained from the following expression involving the fluid temperature and the local axial velocity:

$$T_b = \frac{\int_0^R \rho c_p U T (2\pi r)\, dr}{\rho c_p U_{ax}(\pi R^2)} \tag{2}$$

The average wall heat flux was calculated from the power input and the area of the heating surface. The power input to the test section was determined from the voltage and current measurements. The local Nusselt number and Reynolds number were obtained as

$$\mathrm{Nu} = q_w D/k_f(T_w - T_b) \quad \text{and} \quad \mathrm{Re} = 4\dot{m}_T/\pi D\mu_f \tag{3}$$

where all the properties are evaluated at the bulk temperature. To obtain Reynolds number, the fluid viscosity at the exit bulk temperature is used.

Discussion

Temperature distributions and turbulent flowfield

Figure 4 shows the temperature profiles at various axial locations for initial momentum flux ratio of 2.67. In the figure,

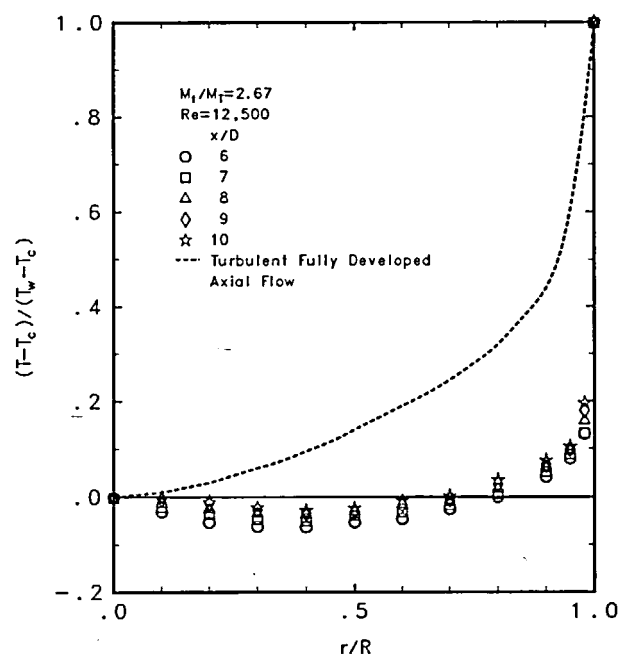

Figure 4 Normalized temperature profile

the temperature differences between the fluid at a radial location and that at the center are normalized by the temperature difference between the wall and the fluid at the center. With heated tube wall, the coldest spot does not occur at the center of the tube. Instead, it occurs at 0.35–0.4 R from the center. It is believed that the temperature near the tube center is higher because in the presence of reverse flow, hot fluid from downstream region is brought upstream. As the swirl decays, the temperature difference between the fluid at the center and that at the coldest spot decreases. The fully developed temperature profile in a purely axial turbulent flow is also plotted as dotted line in Figure 4. It is seen that the temperature profile with swirl is much flatter than the fully developed temperature profile. The flatter profile is probably a result of better mixing, and it corresponds to a higher heat transfer coefficient.

The axial and tangential velocity profiles in a nonisothermal case with an initial momentum flux ratio of 2.67 are plotted in Figures 5 and 6, respectively. The axial velocity has a maximum value near the wall and has a flow reversal region in the core. The tangential velocity profile has a peak value at $r/R = 0.4$–0.6. As swirl decays, the peak value decreases, and the location of the maximum tangential velocity moves toward the center. The maximum axial velocity decreases, and the flow reversal region shrinks with decay in swirl. To assess the effect of heating, the tangential velocity profile at seven hydraulic diameters from the injection location for both the diabatic and adiabatic (Chang and Dhir 1994) flows are shown in Figure 7. It is clear that heating has little effect on the mean flowfield. In a stratified flow, there would exist a significant difference in flowfield between the diabatic flow and the adiabatic flow. However, no such behavior was observed, at least for the wall–bulk temperature difference of less than 30°C.

The bulk temperatures at various axial locations were calculated from the temperature profiles and axial velocity profiles using Equation 2. The difference between the wall temperature and the bulk temperature was found to increase with axial distance, and as such, a reduction in heat transfer coefficient was observed. The local Nusselt number normalized

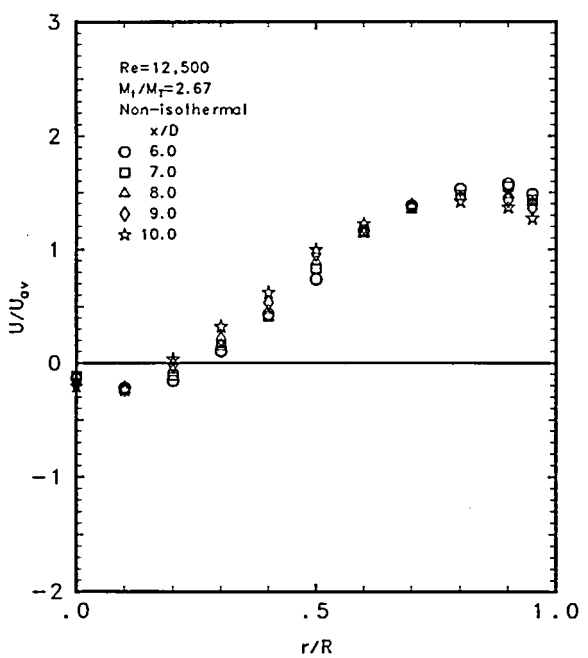

Figure 5 Nonisothermal axial velocity profile

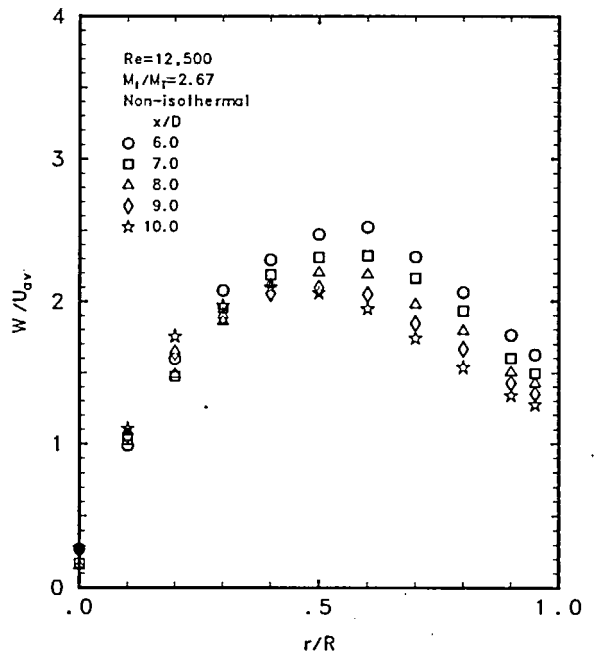

Figure 6 Nonisothermal tangential velocity profile

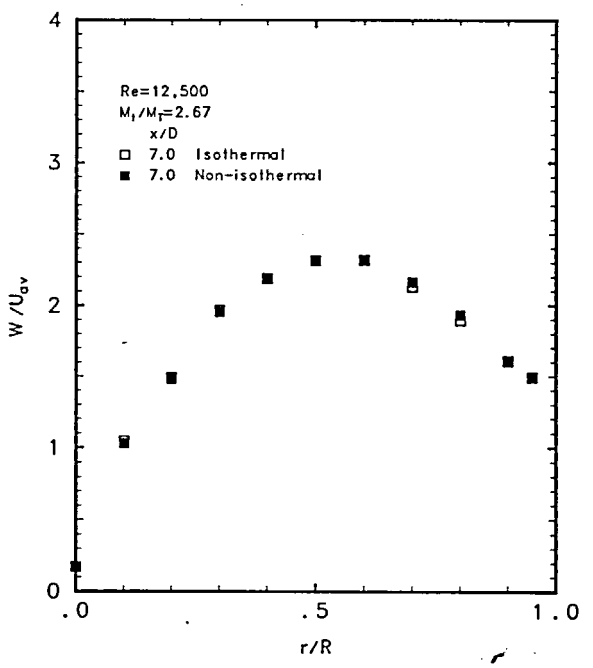

Figure 7 Comparison of tangential velocity profile

by the Nusselt number for fully developed axial flow is plotted in Figure 8. The solid line represents the prediction from the correlation developed by Dhir and Chang (1992). It can be seen the data are consistent with the correlation. The root-mean-square of temperature fluctuations was also measured. Figure 9 shows the radial distribution of the temperature fluctuations. The maximum value of the temperature fluctuation occurs at about 0.5 R and near the wall. The location 0.5 R is near the boundary between forward and reverse flows.

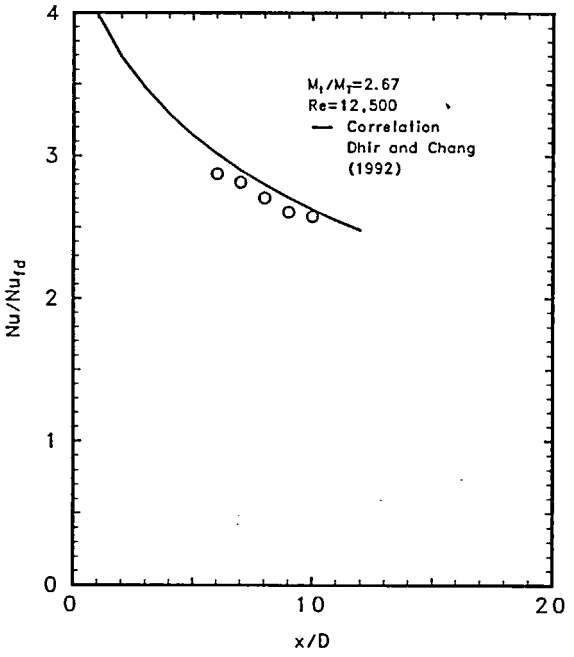

Figure 8 Local Nusselt number in the nonisothermal turbulence measurements

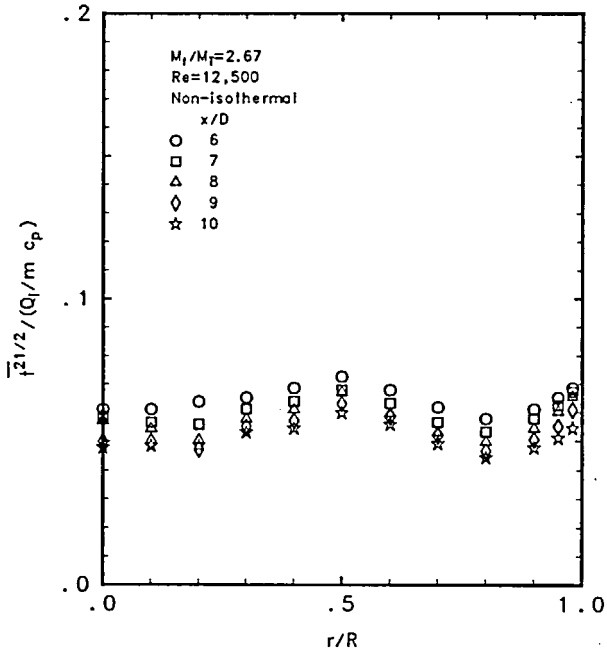

Figure 9 Root-mean-square of the temperature fluctuations

The measured turbulence intensities $\overline{u^2}^{1/2}$, $\overline{v^2}^{1/2}$, and $\overline{w^2}^{1/2}$ for momentum flux ratio of 2.67 are plotted in Figure 10. The turbulence intensities are promoted by the swirl motion significantly and are about 15–20 percent of the bulk velocity. However, the turbulent intensities normalized by the mean total velocity are less than 13 percent for $r/R > 0.1$. As such, the linearization used in evaluating the intensities is valid over most of the tube except in the small core region in the middle. All of the turbulence intensities show a local maximum near $r/R \sim 0.5$. The intensities for all of the components except $\overline{v^2}$ also have a local maximum near the heated wall. No significant change in the turbulence intensities with heating is noticed. The mean square value of twice the energy of turbulence $\overline{q^2}^{1/2}$ can be evaluated from Figure 10. The ratio of the root-mean-square of the temperature fluctuations to that of twice the energy of turbulence is shown in Figure 11. The ratio is quite uniform over the cross-section, although the values near the tube wall and the tube center are a little higher. A nearly flat profile

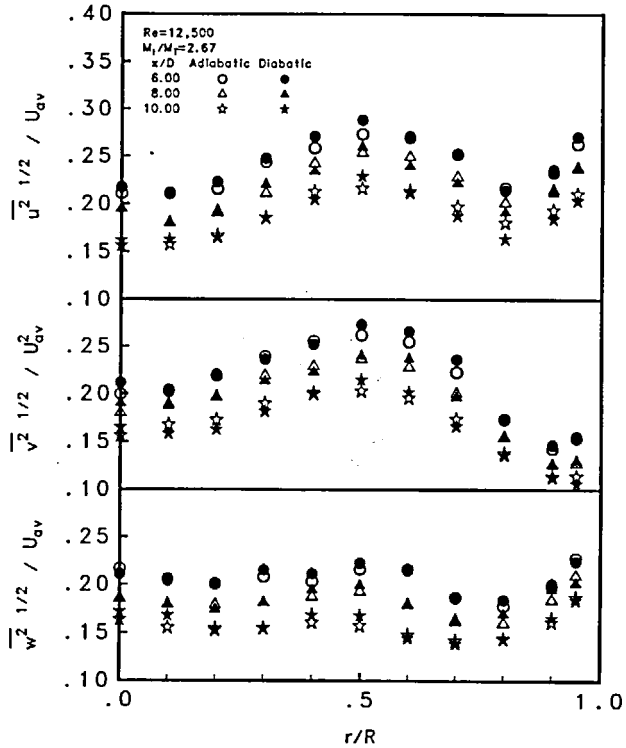

Figure 10 Turbulence intensities

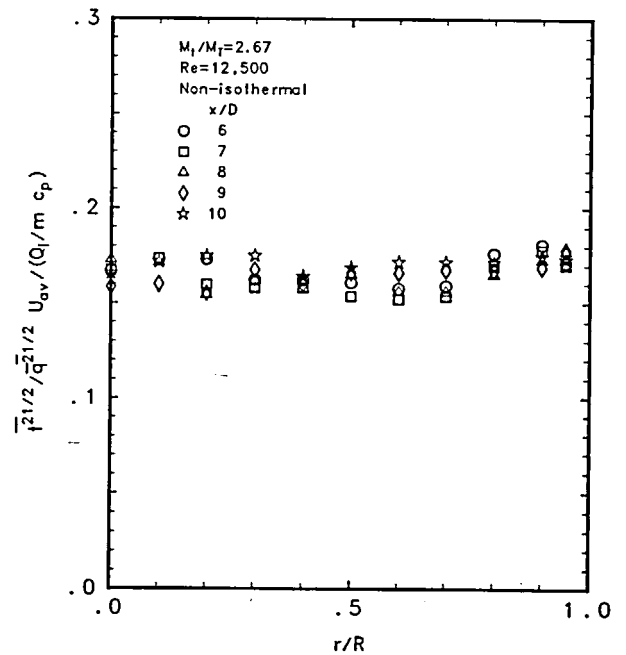

Figure 11 Ratio of the root-mean-square of temperature fluctuations to that of twice the energy of turbulence

implies that the temperature fluctuations and the turbulence intensities have similar behavior in swirl flow.

Figure 12 shows the distributions of Reynolds stress components, $-\overline{uv}$, $-\overline{vw}$, and $-\overline{uw}$, respectively. Comparisons of Reynolds stress components in both adiabatic and diabatic cases shows that no significant difference exists between the isothermal and nonisothermal cases. One possible mechanism of heat transfer enhancement postulated in the past is that the centrifugal force promotes mixing of hot and cold fluids by pushing the cold (heavy) fluid to the wall and hot (light) fluid to the center, when the tube wall is heated. The present experiments show little change in the flowfield, including mean velocities and turbulence quantities when the tube wall is heated. As such, this mechanism is not a major contributor to enhancement in heat transfer, at least in the range of the wall–bulk temperature differences studied in the present experiments.

Mechanisms of heat transfer enhancement

With the exclusion of the centrifugal force caused mixing of hot and cold fluid as a possible mechanism for heat transfer enhancement, the remaining mechanisms are as follows:

(1) The radial pressure gradient resulting from the centrifugal force described in the previous section increases the mean axial velocity near the wall, which leads to higher rates of heat and momentum transfer.
(2) Higher turbulence level promoted by the swirl flow improves the mixing, and thus, the rate of heat transfer.

The relation between the heat transfer enhancement and the swirl intensity can be obtained from the present data, as well as from the earlier work (Dhir and Chang 1992), (Chang and Dhir 1994). Figure 13 shows the heat transfer enhancement as a function of swirl intensity for $x/D \geq 6$. The heat transfer

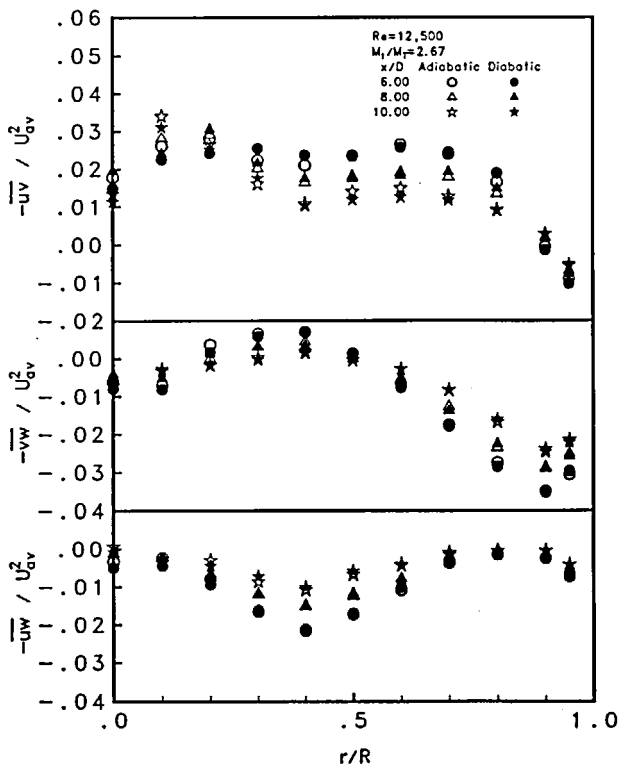

Figure 12 Reynolds stress components

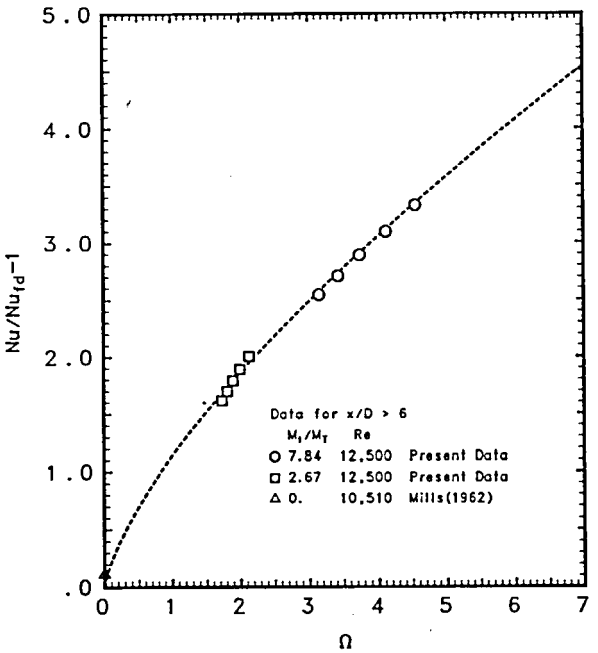

Figure 13 Heat transfer enhancement as a function of swirl intensity

enhancement for a hydrodynamically and thermally developing axial flow (Mills 1962) at six hydraulic diameters from the inlet is also shown in Figure 13. This latter data correspond to $\Omega = 0$. It can be seen that the heat transfer enhancement increases with the swirl intensity. The heat transfer enhancement as a function of the local swirl intensity can be correlated as follows:

$$\frac{\mathrm{Nu}}{\mathrm{Nu}_{fd}} - 1 = 1.14\Omega^{0.71} \quad \text{for} \quad x/D \geq 6 \tag{4}$$

where the swirl intensity Ω is defined as follows:

$$\Omega = \frac{2\pi\rho \int_0^R UWr\,dr}{\rho\pi R^2 U_{av}^2} \tag{5}$$

Data for $x/D \leq 6$ have not been correlated because of the somewhat ambiguous flow conditions near the locations where fluid is injected.

The distribution of the static pressures is evaluated by substituting the tangential and axial velocities in the radial and axial momentum equations and by integrating these equations. The static pressure relative to the wall pressure at a reference location; i.e., at 10 hydraulic diameters from inlet, is plotted in Figure 14. The radial distribution of the static pressure shows that there exists a positive pressure gradient in the core and a negative pressure gradient near the wall. A positive pressure gradient in the core corresponds to a reverse flow in the middle of the tube. As a result, for a given mass flow rate through the tube, the velocity in the forward direction increases in the outer region (near the wall). The enhancement of heat transfer because of increased axial velocity can be assessed by evaluating the dependence of Nusselt number on Reynolds number.

The Nusselt number for fully developed flow in a tube can be correlated as follows (Kays and Crawford 1980):

$$\mathrm{Nu}_{fd} = 0.022\mathrm{Pr}^{0.5}\mathrm{Re}^{0.8} \qquad \mathrm{Re} > 10^5 \tag{6}$$

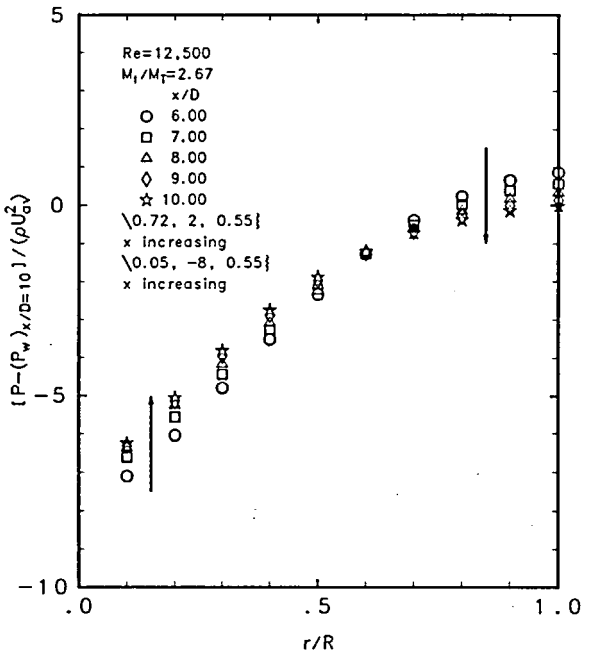

Figure 14 Static pressure

That is, the fully developed Nusselt number is proportional to the 0.8 power of the velocity. Because the heat transfer is proportional to the 0.8 power of the velocity in a purely axial flow, the heat transfer enhancement in swirl flow caused by the increased axial velocity near the wall can be approximately scaled as $(U_{max}/U_{av})^{0.8}$. The ratio of Nusselt number in swirl flow to that in fully developed axial flow scaled by the ratio, $(U_{max}/U_{av})^{0.8}$, is plotted in Figure 15. The heat transfer coefficient observed for a hydrodynamically and thermally developing flow (Mills 1962) at six hydraulic diameters from inlet is also shown in Figure 15 as that corresponding to zero swirl intensity. It is seen that the ratio of heat transfer enhancement with swirl to that caused by the high axial velocity increases with the swirl intensity. Because the ratio is substantially greater than one, all of the enhancement in heat transfer cannot be attributed to increased axial velocity near the wall. It suggests that there must be additional mechanisms for heat transfer enhancement. As seen from Figure 15, initially the enhancement increases very rapidly with swirl intensity. Thereafter, it gradually becomes smaller, as the swirl intensity increases further.

The turbulence intensities shown in Figure 10 have dramatical high values in flow with swirl. For example, the axial turbulence intensities at six hydraulic diameters from the injection location for a momentum flux ratio of 2.67 and a Reynolds number of 12,500 are about 20 percent. The increase of the turbulence intensities is caused by the destabilizing distribution of angular momentum in the free vortex zone and the large shear stress near the boundary of the reversed flow (Chang and Dhir 1994).

Sugawara et al. (1988) investigated the effect of free stream turbulence generated by turbulence grids on heat transfer from a smooth flat plate. They concluded that turbulence in the boundary layer is intensified by the increase of free-stream turbulence intensity. This, in turn, leads to a thickening of the turbulent boundary layer and a thinning of the viscous sublayer. The latter plays a stronger role; hence, heat transfer is enhanced. Sugawara et al.'s (1988) data are plotted in Figure 16. It is seen that heat transfer coefficient increases with increasing turbulence level—rapidly in the range of small turbulence level, and slowly in the high turbulence level range. The solid line is a best fit through the data, and the curve has been extrapolated to higher values of turbulence intensities. At a turbulence level of 7–8 percent, the heat transfer coefficient is about 55 percent higher than that obtained for little or no free-stream turbulence. Because the turbulence level is increased significantly in swirl flow, the heat transfer is expected to be improved. Increased turbulence level could be the other mechanism for enhancement of heat transfer in addition to the increased axial velocity near the wall.

Defining turbulence intensity as follows:

$$Tu = (\overline{u^2})^{1/2}/U_0 \tag{7}$$

the solid line through the data of Sugawara et al. is described by:

$$\mathrm{Nu}/\mathrm{Nu}_0 = 1 + 2.33\,(Tu)^{0.16} \tag{8}$$

The heat transfer enhancement is proportional to 0.16 power of the total turbulence intensity. The average total turbulence intensity over a cross-section in swirl flow can be evaluated as follows:

$$Tu_{av} = \frac{\left[\dfrac{\int_0^R \left(\dfrac{\overline{u^2}+\overline{v^2}+\overline{w^2}}{3}\right)2\pi r\,dr}{\pi R^2}\right]^{1/2}}{U_{av}} \tag{9}$$

Figure 17 shows the average total turbulence intensity as a function of the swirl intensity. The turbulence intensity is correlated as follows:

$$Tu_{av} = 1/\sqrt{3}(0.012 + 0.17\Omega) \tag{10}$$

The Nusselt number valves from Figure 16 along with correlation developed from Figure 17 are combined to estimate as a function of the swirl intensity the heat

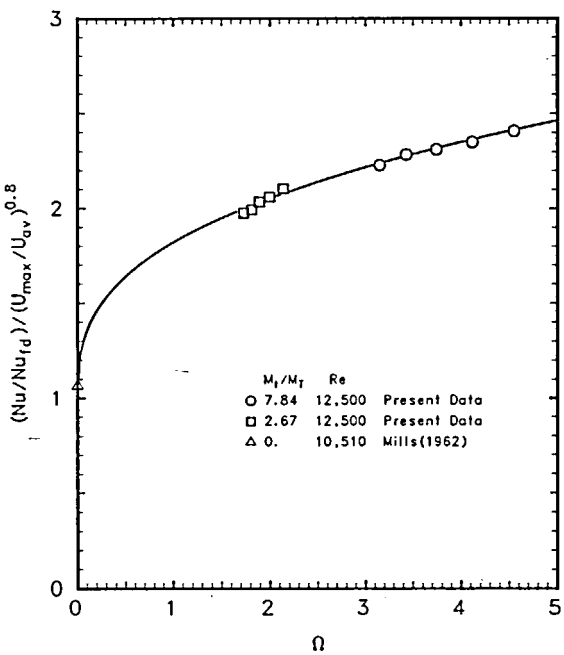

Figure 15 Ratio of the heat transfer enhancement in swirl flow to that attributable to the higher maximum axial velocity

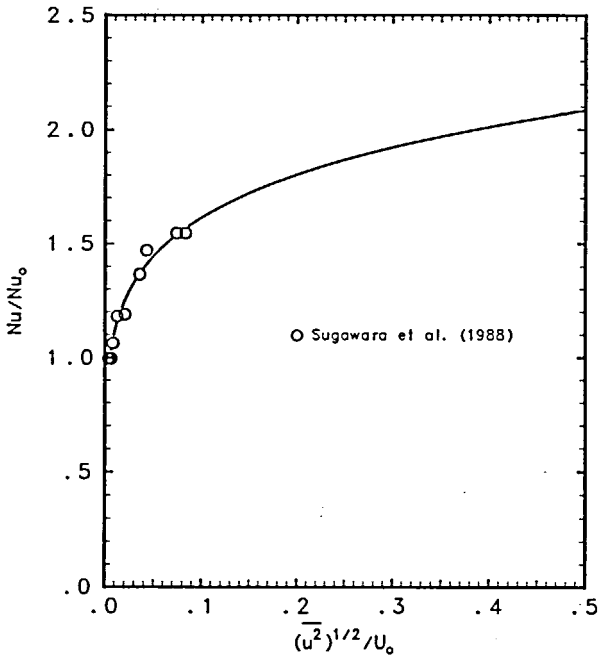

Figure 16 Heat transfer enhancement attributable to the free-stream turbulence level (Sugawara et al. 1988)

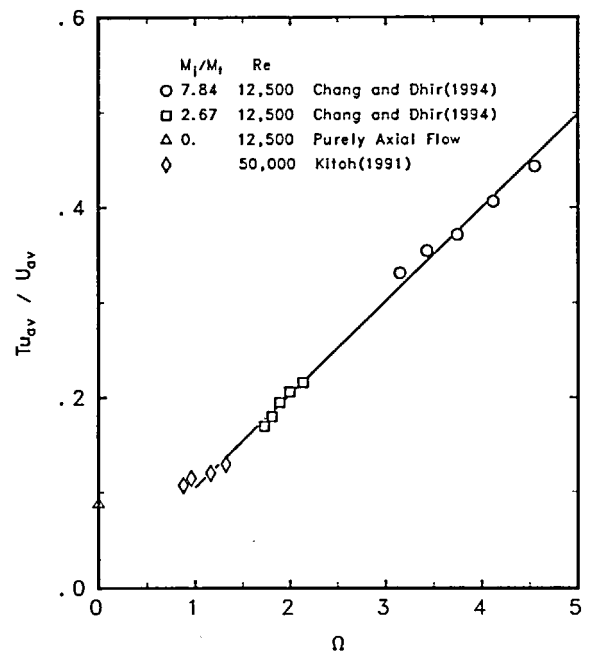

Figure 17 Average turbulence intensity as a function of the swirl intensity

transfer enhancement caused by the turbulence level. Figure 18 shows the heat transfer in swirl flow scaled by the product of heat transfer enhancement caused by the higher maximum axial velocity near the wall, $[(U_{max}/U_{av})^{0.8}]$, and that caused by the intensified turbulence level, $[2.33(Tu_{av})^{0.16}]$. The ratio is close to unity and is nearly independent of swirl intensity. Therefore, it can be concluded that the increased maximum axial velocity near the wall and the intensified turbulence level are the two major mechanisms responsible for the heat transfer enhancement in the tangentially injected swirl flow. Thus, enhancement in heat transfer caused by combined effect of increased velocity and level of turbulence is correlated with swirl intensity as follows:

$$\mathrm{Nu}/\mathrm{Nu}_{fd} = 1.13(U_{max}/U_{av})^{0.8}(2.33Tu_{av}^{0.16})$$
$$= 2.41(1 + 0.24\Omega)^{0.8}(0.012 + 0.17\Omega)^{0.16} \quad (11)$$

Slow decay of the swirl

Swirl introduced at the tube inlet continues to persist for several tens of hydraulic diameters downstream. It has been found (see Chang 1994) that intensity of turbulence is directly related local intensity of swirl; i.e., turbulence level decreases with decay of swirl. Although it is difficult to establish the interacting mechanisms that sustain both the swirl and turbulence intensities over a long distance, Chang (1994) has shown quantitatively that presence of swirl significantly promotes turbulence level. This is caused by the existence of a destabilizing free vortex zone and a large shear stress at the boundary of the forward and reverse flows. The kinetic energy of the mean flow and its decay rate decrease with distance or as the swirl decays. The energy reduction of the mean flow is a direct consequence of turbulence energy production, which, in turn, preserves the turbulence level over a longer distance.

Conclusions

(1) No significant difference in the flowfield and turbulence intensities was found between the adiabatic and the diabatic experiments. Therefore, mixing caused by pushing the colder and heavier fluid to the wall and hotter and lighter fluid to the center as a result of centrifugal force is not considered to be a major mechanism for heat transfer enhancement in the present work in which temperature difference between wall and the bulk fluid was less than 30°C.

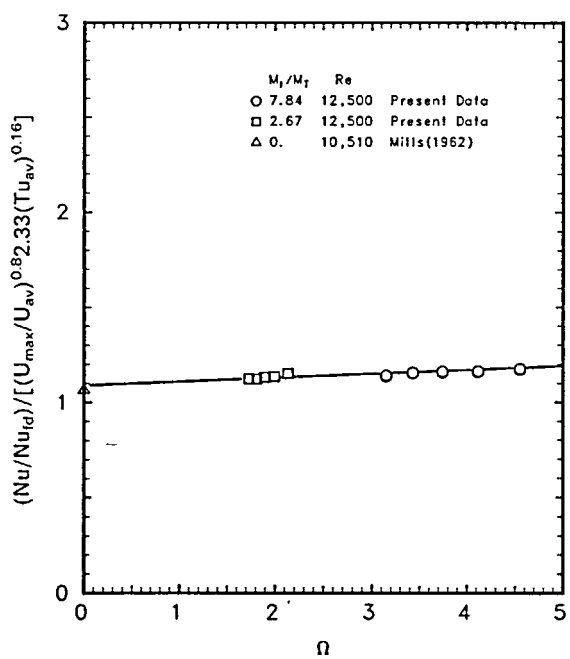

Figure 18 Heat transfer enhancement scaled by that attributable to the two major mechanisms

(2) Two major mechanisms of heat transfer enhancement have been identified and their contributions quantified. The mechanisms are: (1) high axial velocity near the wall increases the wall heat flux; and (2) high turbulence level promotes the mixing and, thus, the heat transfer.
(3) In injection-induced swirl flow, the kinetic energy of the mean flow and its decay rates, and the turbulence level decreases with the axial distance. However, the high turbulence-production is necessary to transfer the kinetic energy of the mean flow to the turbulence energy in a decaying process. The high turbulence- production, in turn, slows down the rate of decrease of the turbulence level.

References

Blackwelder, R. and Kreith, F. 1970. An experimental investigation of heat transfer and pressure drop in a decaying swirl flow. In *Augmentation of Convection Heat and Mass Transfer*. American Society of Mechanical Engineering, New York, 87-93

Barbin, A. R. and Jones, J. B. 1963. Turbulent Flow in the Inlet Region of a Smooth Pipe. *J. Basic Engineering*, pp. 29-34

Bradshaw, P. 1973. *Effects of streamline curvature on turbulent flow*, AGARD-AG-169, NATO-AGARD

Chang, F. 1994. *Experimental and analytical study of heat transfer and turbulent flow field in tangentially injected swirl flow*, Ph.D. Dissertation, University of California, Los Angeles, Los Angeles, CA

Chang, F. and Dhir, V. K. 1994. Turbulent flow field in tangentially injected swirl flows in tubes. *Int. J. Heat Fluid Flow*, **15**, 346–356

Dhir, V. K. and Chang, F. 1992. Heat transfer enhancement using tangential injection. *ASHRAE Trans.*, **98**, 383–390

Guo, Z. and Dhir, V. K. 1987. Effect of injection-induced swirl flow on single and two-phase heat transfer. *ASME HTD*, **81**, 77–84

Kays, W. M. and Crawford, M. E. 1980. *Convective Heat Transfer and Mass Transfer*, McGraw-Hill, New York

Klepper, O. H. 1973. Heat transfer performance of short twisted tapes. *AIChE Symp. Series*, **69**, 87–93

Kreith, F. and Margolis, D. 1959. Heat transfer and friction in turbulent vortex flow. *Appl. Sci. Res.*, **8**, 457-473

Kreith, F. and Sonju, O. K. 1965. The decay of a turbulent swirl in a pipe. *J. Fluid Mech.*, **22**, 257–271

Mills, A. F. 1962. Experimental investigation of turbulent heat transfer in the entrance region of a circular conduit. *J. Mech. Eng. Sci.*, **4**, 63–77

Razgaitis, R. and Holman, J. P. 1976. A survey of heat transfer in confined swirl flows. *Heat and Mass Transfer Proc.*, **2**, 831–866

Sugawara, S., Sato, T., Komatsu, H. and Osaka, H. 1988. Effect of free stream turbulence on flat plate heat transfer. *Int. J. Heat Mass Transfer*, **31**, 5–12

Weske, D. R. and Sturov, G. Ye. 1974. Experimental study of turbulent swirled flows in a cylindrical tube. *Fluid Mech.—Soviet Res.*, **3**, 77–82